Journal of Medicinal Chemistry Article

J. Med. Chem. **2011,** *54,* 201–210 **201**
DOI: 10.1021/jm1010995

Aurora Kinase Inhibitors Based on the Imidazo[1,2-*a*]pyrazine Core: Fluorine and Deuterium Incorporation Improve Oral Absorption and Exposure

Angela D. Kerekes,*[,†] Sara J. Esposite,[†] Ronald J. Doll,[†] Jayaram R. Tagat,[†] Tao Yu,[†] Yushi Xiao,[†] Yonglian Zhang,[†] Dan B. Prelusky,[‡] Seema Tevar,[§] Kimberly Gray,[§] Gaby A. Terracina,[§] Suining Lee,[§] Jennifer Jones,[§] Ming Liu,[§] Andrea D. Basso,[§] and Elizabeth B. Smith[∥]

Departments of [†]Chemical Research, [‡]DMPK, [§]Tumor Biology, and [∥]Discovery Technologies, Merck Research Laboratories, 2015 Galloping Hill Road, Kenilworth, New Jersey 07033, United States

Received August 24, 2010

Aurora kinases are cell cycle regulated serine/threonine kinases that have been linked to cancer. Compound **1** was identified as a potent Aurora inhibitor but lacked oral bioavailability. Optimization of **1** led to the discovery of a series of fluoroamine and deuterated analogues, exemplified by compound **25**, with an improved pharmacokinetic profile. We found that blocking oxidative metabolism at the benzylic position and decreasing the basicity of the amine are important to obtaining compounds with good biological profiles and oral bioavailability.

Introduction

Aurora kinases (Aurora A, B, C) are cell cycle regulated serine/threonine kinases that play a key role in regulating mitosis. Aurora A and B are ubiquitously expressed, while Aurora C is predominantly expressed in the testes.[1] Aurora A and B are frequently overexpressed in various human tumors, including carcinomas of the breast,[2] head and neck,[3] ovary,[4] prostate,[5] bladder,[6] esopagous,[7] thyroid,[8] brain,[9] and colon.[10] This overexpression has been shown to correlate with allelic imbalance, higher clinical grade, tumor invasiness, and poor prognosis.

Aurora kinases are required for cells to properly proceed through mitosis. Aurora A regulates mitotic entry, centromere maturation, bipolar spindle assembly, and chromosome alignment at the metaphase plate. Aurora B regulates chromatin remodeling, kinetochore-spindle attachment, and cytokinesis. Aurora B phosphorylates histone H3 at Ser-10.[11] In turn, inhibition of Aurora results in disruption of the cell cycle and cell death. Thus, disruption of normal Aurora function is expected to impair tumor growth and has potential for broad antitumor activity in a number of cancers.

Published reports demonstrate that single depletion of Aurora A by siRNA results in lagging chromosomes and mitotic defects, while ablation of Aurora B results in polyploidy. Cells in which Aurora B is knocked down have defects in chromosome alignment at metaphase, unequal chromosome segregation at anaphase, followed by a failure to undergo cytokinesis, which results in a cell that is polyploidy (contains >4N DNA content).[12] Furthermore, the chromosomes in the new daughter nuclei are not equally divided; this phenotype cannot be sustained and is followed by cell death. Combination depletion of Aurora A and B by siRNA results in polyploidy, a phenotype identical to single ablation of Aurora B. It appears that Aurora B function is required for the checkpoint induced by loss of Aurora A. Importantly, inhibition of Aurora A does not abrogate or interfere with the phenotypic consequences of Aurora B inhibition.

In earlier studies, imidazopyrazine (**1**) was identified as a potent ATP-competitive Aurora kinase inhibitor (Aurora A $IC_{50} \leq 4$ nM and Aurora B $IC_{50} \leq 13$ nM).[13,14] The X-ray structure of **1** bound to Aurora A, solved at 2.4 Å resolution, is shown in Figure 1.[14] The compound overlaps with the ATP binding site. The N1 and C8-NH groups bind to the Ala 213 in the hinge region. The C3-pyrazole NH acts as a H-donor to Asp 274, and the other pyrazole N acts as a H-bond acceptor from a water molecule. The 6-position is near a hydrophobic region, while the 8-position reached the boundary of the binding cavity and is partially solvent exposed. It was found that modifications in the solvent-exposed region were important for improving the cellular potency. More specifically, a basic nitrogen in the solvent-exposed region was essential for the cellular activity of **1**.[14]

Compound **1** had good aqueous solubility and a favorable profile for intravenous (iv) delivery; however, oral exposures were not achieved with **1**. Earlier studies indicated that the poor oral bioavailability of **1** in rats was due to both rapid metabolism and poor oral absorption. Studies show that 24 h exposure is needed for optimal cell kill.[13] The PK profile of **1** did not support this need; a long infusion would be required in the clinic. Currently, several Aurora inhibitors are being clinically evaluated, many requiring long infusions (www.clinicaltrials.gov). Orally bioavailable compounds should be advantageous. Our goal was to identify orally active Aurora kinase inhibitors in this structural class. Our initial attempt was to prepare prodrugs of **1** with the goal of improving oral absorption.

Both lipophilic and hydrophilic/basic ester prodrugs of **1** were prepared (Scheme 1). The alcohol moiety of **1** was also deriviatized as carbonate and carbamate prodrugs. The pyrazole nitrogen and the C-8 nitrogen were acetylated, and these

*To whom correspondence should be addressed. Phone: 908-740-3659. Fax: 908-740-7441. E-mail: angela.kerekes@merck.com.

Published on Web 12/03/2010

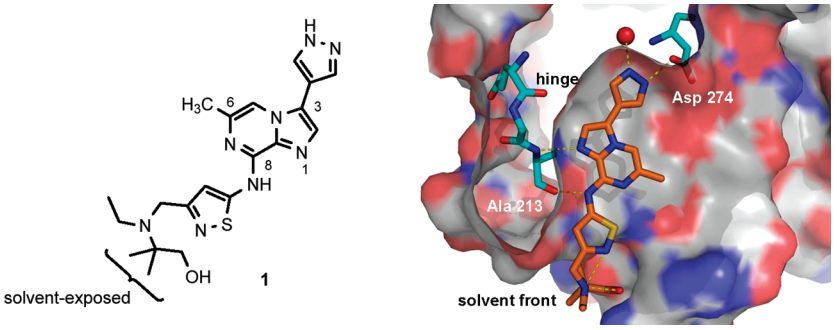

Figure 1. X-ray cocrystal structure of Aurora A and **1**.

Scheme 1. Preparation of Prodrugs of **1**

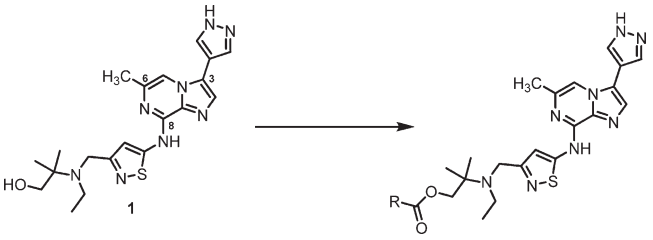

compounds were tested. None of these compounds showed any oral rat pharmacokinetics (PK) when monitoring for both the prodrug and parent compounds (data not shown). After preparing and screening numerous prodrugs of **1**, with no indication of obtaining oral PK, we moved to a new approach.

Radiolabeled metabolite-identification studies for **1** indicated that the major site of metabolism occurs near the basic nitrogen as shown in Scheme 2. The major metabolic pathway is N-dealkylation, with and without oxidation and glucuronidation. Earlier studies showed that this basic nitrogen in the solvent-exposed region is a good place to modulate the physicochemical properties of our inhibitors without losing intrinsic potency.[14] On the basis of this observation, we directed our approach toward blocking metabolism and improving absorption by incorporating fluorine atoms into **1**.

There are many examples in the literature of using fluorine to block metabolism and improve oral absorption.[15−17] Fluorine substitution on both cyclic and linear amines has an inductive effect and lowers the pK_a of the nitrogen, thus lowering the basicity of neighboring amines.[18] These changes in pK_a can affect the physicochemical and ADME (absorption, distribution, metabolism, excretion) properties of a molecule.[19] The two-point strategy was to incorporate fluorine atoms into the solvent-exposed region of **1** to block the observed metabolism and modulate the pK_a of the amine to improve oral absorption.

Chemistry

The synthetic route to fluorinated analogues is shown in Scheme 3. The preparations of **1**, **2**, **5**, **6**, and **15** have been previously described.[14,20] Lithium aluminum hydride reduction of the ester **2** gave the alcohol **3**. The mesylate **4** was formed with methanesulfonyl chloride and triethylamine in dilute THF[a] (0.02 M). The intermediate mesylate **4** was displaced with the fluorinated amino alcohols **5** and **6** and with the commercially available amines shown in Table 2. Crucial to the success of the mesylate displacement reaction was to check the pH of the amines. Amines readily absorb CO_2 in air forming carbonic acid salts. If acidic, a THF solution of the amine was first treated with a base until a basic pH is reached, after which the mesylate **4** and NaI are added to the reaction. The final products (**7**−**23**) were obtained after removal of the SEM protecting group with 4 N HCl in dioxane.

The synthesis of deuterium analogue **25** was straightforward (Scheme 4). Reduction of the methyl ester **2** with $LiAlD_4$ gave a clean reduction to the alcohol. The alcohol was then converted to the mesylate **24** using methanesulfonyl chloride and triethylamine in THF. The mesylate intermediate **24** was displaced with 3,3-difluoropyrrolidine to give **25** after deprotection of SEM group on the C-3 pyrazole.

Results and Discussion

Aurora A and B kinase assays were used to determine the IC_{50} values for the compounds. The detection limits for these assays are 4 nM for Aurora A and 13 nM for Aurora B, as the assays utilize 8 and 26 nM enzyme, respectively. The mechanism-based cellular activity was determined by assessing the loss of phosphorylation of histone H3 (phos-HH3), a specific marker for Aurora B activity.[21]

The difluoroethyl (**7**) and trifluoroethyl (**8**) analogues of **1** were prepared. Compounds **1**, **7**, and **8** had potent biochemical activity for both Aurora A and B (Table 1). A 10-fold loss in cellular potency (phos-HH3) in the fluorinated analogues **7** and **8** was observed compared to **1**. This loss in cellular potency is possibly due to the decrease in amine basicity with the addition of fluorine atoms. Each additional fluorine atom decreases the basicity of the amine by ~1.7 pK_a units,[18] thus possibly affecting cellular potency. A considerable improvement is seen in the oral rat AUC (area under curve) of **8** compared to **1**, possibly due to inhibition of the *N*-ethyl metabolism. These results indicated that by incorporation of fluorine into our compounds, the oral PK could be improved with this class of compounds.

[a] Abbreviations: THF, tetrahydrofuran; SEM, 2-(trimethylsilyl)-ethoxymethyl; TFA, trifluoroacetic acid; HPBCD, hydroxylpropyl β-cyclodextrin; MC, methylcellulose; mpk, milligrams per kilogram; CHK1, checkpoint kinase 1; EPHB4, ephrin type B receptor 4; FLT3, fms-like tyrosine kinase receptor 3; IRAK4, interleukin-1 receptor-associated kinase 4; KDR, kinase insert domain receptor; LCK, lymphocyte-specific protein tyrosine kinase; AKT1, *v*-akt murine thymoma viral oncogene homologue; CAMK4, calcium/calmodulin-dependent protein kinase type 4; CDK2, cyclin-dependent kinase 2; CSNK1D, casein kinase 1 isoform δ; EGFR, epidermal growth factor receptor; ERK2, extracellular signal-regulated kinase; IGF1R, insulin-like growth factor 1 receptor; IKKB, 1κB kinase β; JAK2, Janus activated kinase 2; MET, hepatocyte growth factor receptor; MST2, mammalian sterile 20-like kinase 2; NEK2, never in mitosis gene A-related kinase; PKCA, protein kinase Cα; PLK3, polo-like kinase 3; ROCK2, Rho-associated coiled-coil containing protein kinase 2; RSK2, p90 ribosomal S6 kinase; TSSK2, testis-specific serine/threonine protein kinase 2.

Scheme 2. Metabolite Characterization of ^{3}H-**1**

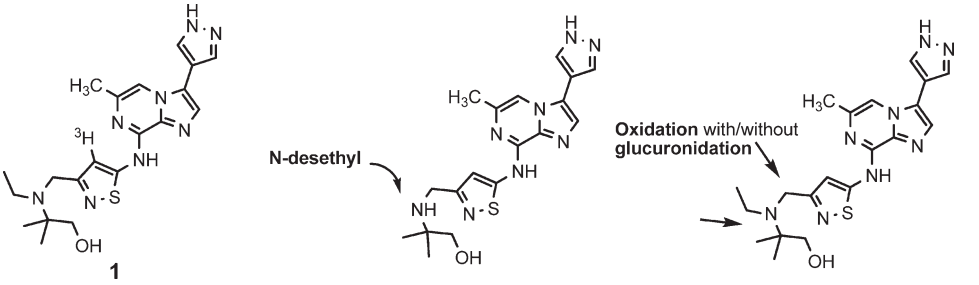

Scheme 3[a]

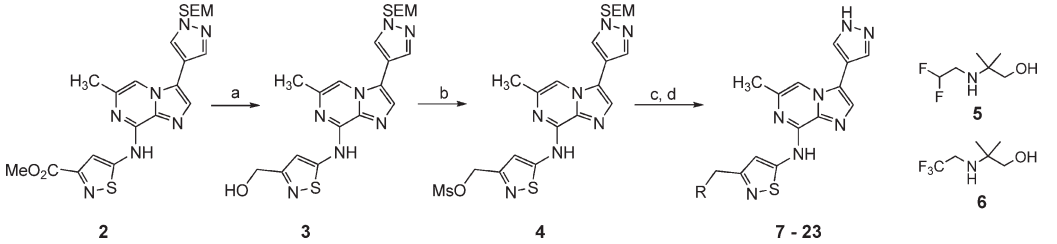

[a] Reagents and conditions: (a) $LiAlH_4$, THF, room temp (57%); (b) MsCl, Et_3N, THF (0.02 M), room temp, 5 min (65%); (c) **5**, **6**, or amines in Table 2, NaI, THF, 80 °C; (d) 4 N HCl/dioxane, THF/MeOH (1:1), 80 °C.

Scheme 4[a]

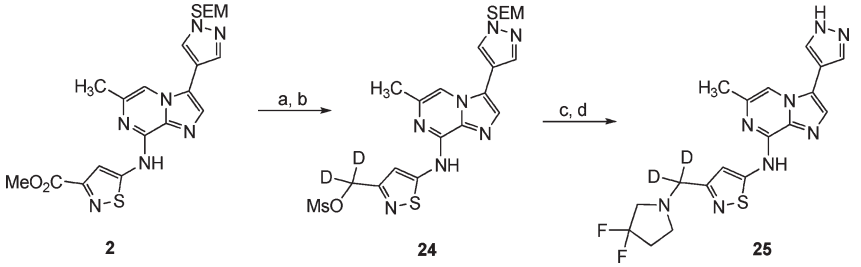

[a] Reagents and conditions: (a) $LiAlD_4$, THF, room temp (49%); (b) MsCl, Et_3N, THF (0.02 M), room temp, 5 min (62%); (c) 3,3-difluoropyrrolidine, NaI, THF, 80 °C; (d) 4 N HCl/dioxane, THF/MeOH (1:1), 80 °C (69%, two steps).

Table 1. Effects of Fluorine Substitution on Potency and Oral PK

Cmpd #	Structure	Aurora A IC_{50} (nM)	Aurora B IC_{50} (nM)	phos-HH3[a] IC_{50} (nM)	Rat PK[b] AUC (μM·h)
1	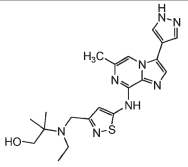	≤ 4	≤ 13	25	0
7	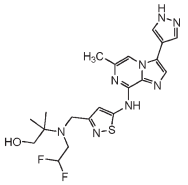	≤ 4	≤ 13	306	0.28
8	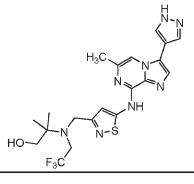	≤ 4	≤ 13	198	0.86

[a] phos-HH3 = phosphorylation of histone H3 in HCT116. [b] $AUC_{(0-6h)}$. Data are from pooled samples from rats (n = 2, 10 mpk, po 20% HPBCD) in a rapid rat protocol; see ref 22.

Table 2. Profile of Fluorinated Amine Analogues

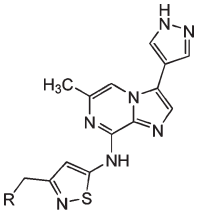

Cmpd #	R	Aurora A IC_{50} (nM)	Aurora B IC_{50} (nM)	phos-HH3[a] IC_{50} (nM)	Rat PK[b] AUC (μM·h)
9		≤ 4	≤ 13	45	0.21
10	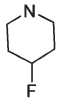	≤ 4	≤ 13	86	2.20
11		≤ 4	≤ 13	74	0.95
12		≤ 4	≤ 13	193	1.21
13		≤ 4	≤ 13	79	1.56
14	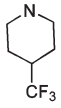	≤ 4	≤ 13	218	1.34
15		≤ 4	≤ 13	88	0
16		≤ 4	≤ 13	93	0.76
17		≤ 4	≤ 13	82	0.74
18		≤ 4	≤ 13	91	1.61
19		≤ 4	≤ 13	50	0.11
20[c]		≤ 4	≤ 13	191	0.18
21		≤ 4	≤ 13	76	12.07
22	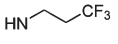	≤ 4	≤ 13	63	10.88
23	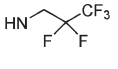	≤ 4	≤ 13	51	3.42

[a] phos-HH3 = phosphorylation of histone H3. [b] $AUC_{(0-6h)}$, 10 mpk (20% HPBCD), po. [c] Trifluoroacetate salt.

The next approach was to prepare fluorinated analogues of compounds bearing various amine substituents at the benzylic position of the isothiazole ring. The biological data and oral exposure level (AUC) in rat for these compounds are shown in Table 2. All compounds were tested as hydrochloride salts unless otherwise specified. The nonfluorinated piperidine **9** is a compound previously shown to have antitumor efficacy when dosed intraperitoneal. When tested for oral PK in rats, **9** displayed modest levels of drug exposure (AUC = 0.2 μM·h). It was decided that **9** was a reasonable starting point, and fluorinated cyclic amines were explored in order to build in oral bioavailability.

Table 3. Pharmacokinetic Data for Selected Compounds[a]

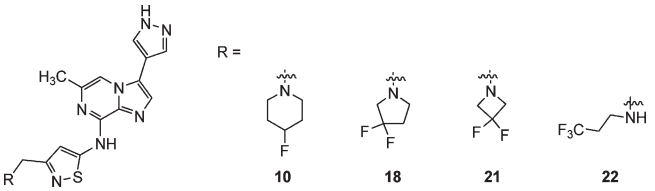

parameter	compd 10	18	21	22
	Mouse[b,c]			
oral AUC (50 mpk, po)	1.2	9.4	7.1[d]	11.1
bioavailability (%)	10	60	nt	nt
	Rat[c,e]			
oral AUC (30 mpk, po)	8.0	6.9	7.1	20.5
bioavailability (%)	21	19	12	22
	Dog[c,e]			
oral AUC (10 mpk, po)	6.1	2.6	3.8	0.3
bioavailability (%)	38	20	nt	nt
	Monkey[c,e]			
oral AUC (10 mpk, po)	0.4	0.8	0.1	0.03
bioavailability (%)	3	2	nt	nt

[a] nt = not tested. [b] Dosed in 20% HPBCD. [c] $AUC_{(0-24h)}$ in $\mu M \cdot h$. [d] Trifluoroacetate salt. [e] Dosed in 0.4% MC.

Table 4. Rat in Vivo Clearance

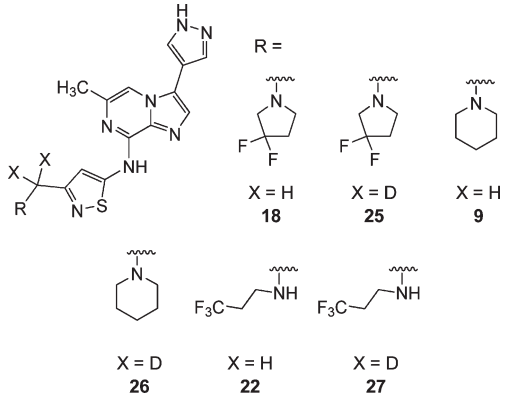

	compd 18	25	9	26	22	27
clearance[a]	33	6.3	80	35	12	5.1

[a] Plasma clearance [(mL/min)/kg].

All compounds in Table 2 showed good Aurora A and B enzyme inhibition. Most compounds displayed $IC_{50} < 100$ nM in our cellular assay (phos-HH3), the exceptions being compounds **12**, **14**, **20**. The fluorinated piperidine analogues, **10**−**13**, showed a 5- to 10-fold improvement in rat oral plasma exposures but a 2- to 4-fold loss in cellular potency compared to **9**.

Fluorinated pyrrolidine analogues **16**−**19** were evaluated. The nonfluorinated pyrrolidine **15** showed no oral exposures in rat. The monofluoro enantiomers **16** and **17** had good potencies but still limited rat plasma exposures. The 3,3-difluoropyrrolidine analogue **18** showed moderate improvement in exposure in rat and better overall potency. However, the tetrafluoropyrrolidine **19** had very poor oral PK. Fluorine

Table 5. Profile of Deuterated Amine Analogue **25**

compd	Aurora A IC_{50} (nM)	Aurora B IC_{50} (nM)	phos-HH3[a] IC_{50} (nM)	rat oral PK[b] AUC ($\mu M \cdot h$)
25	≤4	≤13	63	4.73
18	≤4	≤13	91	1.61

[a] phos-HH3 = phosphorylation of histone H3. [b] $AUC_{(0-6h)}$, 10 mpk (20% HPBCD), po.

Table 6. Pharmacokinetic Profile of **25** and **18**[a]

parameter	compd 25	18
	Mouse[b]	
AUC (3 mpk, iv)	5.9	0.9
clearance [(mL/min)/kg]	20.3	127
AUC (50 mpk,po)	35.9	9.4
bioavailability (%)	37	60
	Rat	
AUC[b] (10 mpk, iv)	63.3	12.2
clearance [(mL/min)/kg]	6.3	33
AUC[c] (30 mpk, po)	62.1	6.9
bioavailability (%)	33	19
	Dog	
AUC[b] (iv)	9.0 (1 mpk)	0.4 (0.3 mpk)
clearance [(mL/min)/kg]	4.5	31
AUC[c] (10 mpk, po)	3.1	2.6
bioavailability (%)	33	20
	Monkey	
AUC[b] (iv)	9.5 (1 mpk)	0.7 (0.3 mpk)
clearance [(mL/min)/kg]	4.2	18
AUC[c] (30 mpk, po)	5.1	1.7
bioavailability (%)	2	2

[a] PK: $AUC_{(0-24h)}$ $\mu M \cdot h$. [b] Dosed in 20% HPBCD. [c] Dosed in 0.4% MC.

introduction on the pyrrolidine ring did not seem to have a negative effect on cellular potency. The difluoroazetidine analogue **21** had potent cellular activity and a significant increase in plasma exposure following oral dosing to rat (AUC = 12.1 $\mu M \cdot h$). The incorporation of fluorine atoms into noncyclic secondary amines was also explored. The fluorinated secondary amines (**22**, **23**) showed potent cellular activities and reasonable rat oral PK (AUC = 10.88 and 3.42 $\mu M \cdot h$, respectively).

Four compounds (**10**, **18**, **21**, and **22**) were chosen to further profile in mouse (CD-1), rat (Sprague−Dawley), dog (beagle), and monkey (cynomolgus) oral PK studies and these pharmacokinetic data are shown in Table 3.

Compounds **10**, **18**, and **21** (Table 3) showed good oral exposure in mouse, rat, and dog. However, all compounds had a poor PK profile in monkey. Azetidine **21** was not evaluated further because of poor chemical stability. The difluoroazetidine ring is susceptible to nucleophilic ring-opening. The secondary fluorinated amine analogue **22** showed good oral exposures in rodents; however, poor oral exposures were observed in dog and monkey. On the basis of the above data, additional modifications of this class of compounds were needed to enhance the overall PK profile.

The in vitro metabolic profile of ^3H-labeled **18** in human and monkey hepatocytes indicated benzylic oxidation (next to the isothiazole ring). In an attempt to block this type of metabolism, the effect of geminal, benzylic deuteration was investigated. Carbon−deuterium bonds are stronger than carbon−hydrogen bonds, and the replacement of hydrogen atoms at metabolically labile sites with deuterium atoms can

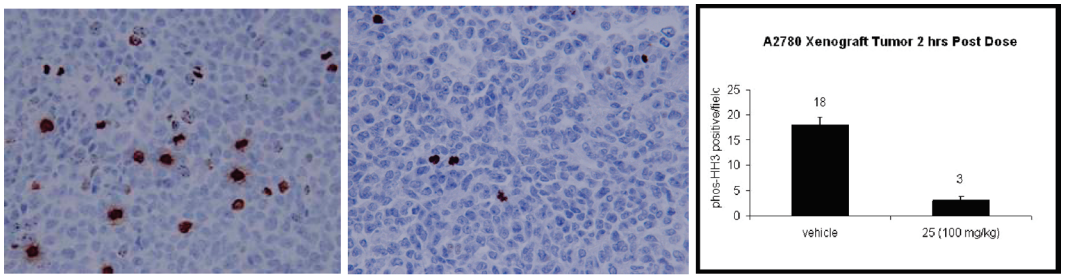

Vehicle (20% HPBCD)[a] **25** (100 mpk, *p.o.*)[a]

Figure 2. Compound **25** decreases levels of phos-HH3 in A2780 tumor xenografts. The footnote "a" indicates 2 h postdose at 40× magnification.

Table 7. Kinase Selectivity of Fluorine and Deuterium Analogues

kinase[a]	**1** IC_{50} (nM)	**18** IC_{50} (nM)	**25** IC_{50} (nM)
CHK1	13	640	200
EPHB4	100	770	700
FLT3	5	76	46
IRAK4	8	1000	640
KDR	< 1	550	340
LCK	< 1	2353	470

[a] Kinases with $IC_{50} < 100$ nM out of 23 kinases tested. Other kinases tested ($IC_{50} > 100$ nM): AKT1, CAMK4, CDK2, CSNK1D, EGFR, ERK2, IGF1R, IKKB, JAK2, MET, MST2, NEK2, PKCA, PLK3, ROCK2, RSK2, TSSK2.

result in a slower metabolism due to the kinetic isotope effect.[23] Many of the geminal, benzylic deuterium analogues of the compounds shown in Tables 1 and 2 were prepared and screened. The enzymatic and cellular potencies of the deuterium analogues were comparable to those of their corresponding nondeuterated analogues displayed in Tables 1 and 2. Not all deuterium analogues showed an improvement in rat oral exposures. For the compounds that did show an improvement in oral rat exposures, upon further evaluation, an improvement in the rat in vivo clearance was found. Table 4 shows a comparison of the PK data for some selected deuterated and nondeuterated analogues. A 2- to 5-fold decrease in the clearance rate is observed. This indicated that the incorporation of deuterium atoms at the benzylic site blocked metabolism.

Compound **25**, the deuterated analogue of **18**, had the best overall profile (Table 5 and 6). Compound **25** has improved cellular potency and oral exposure in rats compared to **18** (Table 5).

The deuterated analogue **25** has good exposure and reasonable bioavailability in mouse, rat, and dog (Table 6). There was a 3-fold improvement in the oral monkey exposure of **25** compared to **18**. Additionally, compound **25** shows a 5- to 6-fold reduction of in vivo clearance in all species, compared to **18**.

The pharmacodynamic marker, phosphorylation of histone H3, was used to profile **25** in vivo. In tumor cell lines the compound rapidly inhibited phosphorylation of histone H3 at serine-10, an indication of Aurora B kinase inhibition. In vivo, inhibition of histone H3 phosphorylation by **25** was assessed by analyzing changes in A2780 human ovarian tumor xenografts grown in nude mice (Figure 2). Animals were dosed orally with **25** at 100 mg/kg, and percent inhibition of histone H3 phosphorylation was determined by comparing the levels in tumors between vehicle and compound-treated mice. As a single agent, **25** inhibited phosphorylation of histone H3. Two hours after a single po dose of **25** at 100 mg/kg resulted in inhibition of the biomarker by 83%.

These deuterium and fluoroamine analogues, including **25**, have an improved kinase selectivity profile compared to **1**. When evaluated in a panel of 23 kinases, **1** displayed activity ($IC_{50} \leq 100$ nM) against 6 of the 23 kinases (Table 7). Compounds **18** and **25** only inhibited Flt3, a hematopoietic growth factor receptor, out of the 23 kinases tested. Flt3 is also inhibited by several structurally diverse Aurora kinase inhibitors, many that are currently in the clinic.[24]

Conclusions

The incorporation of fluorine substituents affects metabolism, amine pK_a, and physicochemical properties, impacting cell activity, oral absorption, and exposure. Oral exposure, across multiple species, can be achieved by blocking metabolism and by modulating the pK_a of the amine in the solvent-exposed region of the imidazopyrazine class of compounds. Blocking metabolism and modulating the physicochemical properties by incorporating fluorine and deuterium atoms enabled us to obtain oral exposures in multiple species within this structural class of compounds. Deuterium incorporation yielded a reduction in the clearance across all species tested and a 3-fold improvement in oral exposure in monkey. We have identified compound **25** as a potent, orally available Aurora kinase inhibitor with an attractive in vitro and in vivo profile. Through the identification of **25** we have applied this approach to other types of amines, and the effects on oral PK will be reported in due course.

Experimental Section

General Methods. Analytical thin-layer chromatography (TLC) was performed on Analtech precoated silica gel plates. NMR spectra were recorded at 400 MHz for ^1H and at 125 MHz for ^{13}C on a Bruker or Varian spectrometer with CD_3OD, $CDCl_3$, or DMSO-d_6 as solvent. The chemical shifts are given in ppm, referenced to the deuterated solvent signal. Purity of target compounds was determined using LC−MS analysis, performed using an Applied Biosystems API-150 mass spectrometer and Shimadzu SCL-10A LC system (column, Phenomenex Gemini C18, 5 μm, 50 mm × 4.6 mm i.d.; gradient from 90% water, 10% CH_3CN, 0.05% TFA, 5 min, to 5% water, 95% CH_3CN, 0.05% TFA in 5 min; UV detection at 254 nm). All target compounds were >95% pure unless otherwise stated. HRMS information was determined using a JEOL Accuo-ToF instrument in positive ESI mode. All compounds are within an error of 1.4×10^{-3} ppm for the elemental composition. The preparation of **1**, **2**, **5**, **6**, and **15** has been previously described.[14,20] All commercially available amines were used as received.

(5-(6-Methyl-3-(1-((2-(trimethylsilyl)ethoxy)methyl)-1*H*-pyrazol-4-yl)imidazo[1,2-*a*]pyrazin-8-ylamino)isothiazol-3-yl)methanol (3). A flask was charged with lithium aluminum hydride (1.23 g,

32.4 mmol). Anhydrous THF was added (50 mL). A solution of **2** (3.03 g, 6.25 mmol) in anhydrous THF (100 mL) was carefully added to the reaction flask. The resulting mixture was stirred at room temperature under a N_2 atmosphere for 1.0 h. The reaction was carefully quenched by the sequential addition of 1.23 mL of H_2O, 1.23 mL of 15% NaOH (aq), and 3.7 mL of H_2O. After being stirred for 10 min, the mixture was filtered through a very thin pad of Celite (rinsing with THF). Concentration of the filtrate yielded a light yellow solid. Triturating with MeOH gave pure **3** (1.62 g, 57% yield) as a white solid. ^{1}H NMR (400 MHz, DMSO-d_6) δ 12.0 (s, NH), 8.61 (s, 1H), 8.11 (s, 1H), 7.88 (broad s, 2H), 7.18 (s, 1H), 5.51 (s, 2H), 5.34 (broad s, OH), 4.45 (d, J = 5.6 Hz, 2H), 3.62 (t, J = 8.0 Hz, 2H), 2.45 (s, 3H), 0.88 (t, J = 8.0 Hz, 2H), 0.0 (s, 9H); mass calculated for formula $C_{20}H_{27}N_7O_2SSi$ 457.2; observed MH^+ (LCMS) 458.4 (m/z); ^{13}C NMR (125 MHz, $CDCl_3$) δ 166.3, 162.0, 142.3, 139.1, 137.6, 132.0, 131.6, 128.4, 120.8, 110.7, 107.6, 105.7, 81.1, 67.8, 62.8, 20.9, 18.3, −1.0 (3C); HRMS (ESI) m/z obsd 458.1793 (M + H), calcd 458.1794.

(5-(6-Methyl-3-(1-((2-(trimethylsilyl)ethoxy)methyl)-1*H*-pyrazol-4-yl)imidazo[1,2-*a*]pyrazin-8-ylamino)isothiazol-3-yl)methyl Methanesulfonate (4). A solution of the alcohol **3** (1.99 g, 4.35 mmol) in THF (220 mL) was treated with Et_3N (2.06 mL, 14.8 mmol) followed by methanesulfonyl chloride (0.84 mL, 6.90 mmol). The mixture was stirred at room temperature for 5 min, and then water (100 mL) was added. Dichloromethane (200 mL) was added, and the layers were separated. The organic phase was washed with 1.0 N HCl (aq), saturated $NaHCO_3$ (aq), and brine. The organic phase was dried over Na_2SO_4, filtered, and concentrated in vacuo to give an off-white solid. Triturating with MeOH gave pure **4** (1.53 g, 65% yield) as a white solid. ^{1}H NMR (400 MHz, $CDCl_3$) δ 10.5 (broad s, NH), 7.92 (s, 1H), 7.84 (s, 1H), 7.65 (s, 1H), 7.54 (s, 1H), 7.03 (s, 1H), 5.55 (s, 2H), 5.28 (s, 2H), 3.68 (t, J = 8.4 Hz, 2H), 3.04 (s, 3H), 2.54 (s, 3H), 0.97 (t, J = 8.4 Hz, 2H), 0.01 (s, 9H); mass calculated for formula $C_{21}H_{29}N_7O_4S_2Si$ 535.2; observed MH^+ (LCMS) 536.3 (m/z); ^{13}C NMR (125 MHz, $CDCl_3$) δ 162.7, 158.9, 142.0, 139.1, 138.1, 131.4, 130.8, 128.9, 121.2, 110.1, 107.8, 107.4, 81.1, 68.3, 67.8, 38.6, 20.9, 18.3, −1.0 (3C); HRMS (ESI) m/z obsd 536.1563 (M + H), calcd 536.1570.

General Procedure. 2-[(2,2-Difluoroethyl)[[5-[[6-methyl-3-(1*H*-pyrazol-4-yl)imidazo[1,2-*a*]pyrazin-8-yl]amino]-3-isothiazolyl]methyl]-amino]-2-methyl-1-propanol Hydrochloride (7). To a solution of **5** (0.14 g, 0.94 mmol) in THF (4 mL) was added NaH (55.1 mg, 1.38 mmol, 60% dispersion in mineral oil). The mixture was stirred under a N_2 atmosphere at room temperature for 10 min. The pH was checked to ensure that the reaction is mildly basic. The mesylate **4** (98.6 mg, 0.18 mmol) and NaI (15.4 mg, 0.10 mmol) were added to the reaction flask. The mixture was heated at 80 °C under a N_2 atmosphere for 8 h. The mixture was cooled to room temperature, and 15 mL of saturated aqueous NH_4Cl solution was added. The mixture was diluted with dichloromethane, and the layers were separated. The aqueous layer was extracted with dichloromethane (2 × 20 mL). The organic phase was washed with 15 mL of saturated aqueous $NaHCO_3$, then brine (15 mL). The organic phase was dried over Na_2SO_4 and concentrated in vacuo. Purification via preparative TLC (10% MeOH/CH_2Cl_2) gave 32.6 mg (30% yield). A solution of this compound in THF/MeOH (0.27 mL/0.27 mL) was immersed in a preheated oil bath at 80 °C. A solution of 4 N HCl/dioxane (0.27 mL, 1.10 mmol) was added via syringe to the reaction flask. The mixture was stirred at 80 °C for 30 min. Tetrahydrofuran (1.1 mL) was added, and the mixture was cooled to room temperature. The precipitated solid was collected by filtration, washed with THF (10 mL), then Et_2O (25 mL), and dried under vacuum to give 29.5 mg (99% yield) of an off-white solid (**7**). ^{1}H NMR (400 MHz, CD_3OD) δ 8.26 (app bs, 2H), 8.14 (s, 1H), 8.09 (s, 1H), 7.28 (s, 1H), 6.40 (t, J = 54.8 Hz, 1H), 4.85 (s, 2H), 3.73 (s, 2H), 3.61 (t, J = 15.8 Hz, 2H), 2.65 (s, 3H), 1.66 (s, 6H); mass calculated for formula $C_{20}H_{24}F_2N_8OS$ 462.5; observed MH^+ (LCMS) 463.3 (m/z), 91% pure by LCMS; ^{13}C NMR (125 MHz, DMSO-d_6) δ 163.6, 162.4, 151.3, 141.7, 137.3, 133.1, 130.5, 129.2, 122.7, 114.0 (t, J = 238 Hz), 109.2, 108.1, 107.4, 73.6, 70.4, 60.4, 43.6 (t, J = 25 Hz), 21.5 (2C), 20.7; HRMS (ESI) m/z obsd 463.1761 (M + H), calcd 463.1762.

2-Methyl-2-[[[5-[[6-methyl-3-(1*H*-pyrazol-4-yl)imidazo[1,2-*a*]pyrazin-8-yl]amino]-3-isothiazolyl]methyl](2,2,2-trifluoroethyl)amino]-1-propanol Hydrochloride (8). Following the general procedure, using amine **6** gave 32.4 mg (59%, two-step yield) of the title compound (**8**) as a white solid. ^{1}H NMR (400 MHz, CD_3OD) δ 8.35 (bs, 2H), 8.21 (s, 2H), 8.13 (s, 1H), 7.32 (s, 1H), 4.15−4.09 (m, 2H), 3.80−3.60 (m, 2H), 3.66 (s, 2H), 2.66 (s, 3H), 1.50 (s, 6H); mass calculated for formula $C_{20}H_{23}F_3N_8OS$ 480.5; observed MH^+ (LCMS) 481.3 (m/z); ^{13}C NMR (125 MHz, DMSO-d_6) δ 163.6, 162.4, 152.8, 141.6, 137.5, 133.1, 130.3, 129.6 (q, J = 188 Hz), 125.3, 122.7, 109.2, 108.0, 107.4, 73.3, 70.3, 61.3, 42.8 (q, J = 38 Hz), 21.6 (2C), 20.7; HRMS (ESI) m/z obsd 481.1745 (M + H), calcd 481.1746.

6-Methyl-*N*-[3-(1-piperidinylmethyl)-5-isothiazolyl]-3-(1*H*-pyrazol-4-yl)imidazo[1,2-*a*]pyrazin-8-amine Hydrochloride (9). Following the general procedure, only substituting **5** with piperidine, compound **9** was obtained in a 20% yield over two steps. ^{1}H NMR (400 MHz, DMSO-d_6) δ 10.6 (broad s, NH), 8.30 (app s, 2H), 8.25 (s, 1H), 8.13 (s, 1H), 7.43 (s, 1H), 4.37−4.36 (m, 2H), 3.40−3.37 (m, 2H), 3.02−2.90 (m, 2H), 2.52 (s, 3H), 1.81−1.75 (m, 4H), 1.70−1.36 (m, 2H); mass calculated for formula $C_{19}H_{22}N_8S$ 394.5; observed MH^+ (LCMS) 395.2 (m/z); ^{13}C NMR (125 MHz, DMSO-d_6) δ 162.7, 156.6, 152.1, 140.9, 138.9, 133.5, 129.1, 126.2, 122.8, 110.3, 109.3, 107.3, 56.1, 53.1 (2C), 23.1 (2C), 22.1, 20.7; HRMS (ESI) m/z obsd 395.1758 (M + H), calcd 395.1766.

***N*-[3-[(4-Fluoro-1-piperidinyl)methyl]-5-isothiazolyl]-6-methyl-3-(1*H*-pyrazol-4-yl)imidazo[1,2-*a*]pyrazin-8-amine Hydrochloride (10).** Following the general procedure, only substituting **5** with 4-fluoropiperidine hydrochloride, gave 1.41 g (51%, two-step yield) of the title compound (**10**) as a tan solid. ^{1}H NMR (400 MHz, CD_3OD) δ 8.33−8.32 (m, 3H), 8.12 (s, 1H), 7.40 (s, 1H), 5.07−4.90 (m, 1H), 4.52 (s, 2H), 3.74−3.38 (m, 4H), 2.65 (s, 3H), 2.40−2.00 (m, 4H). Mass calculated for formula $C_{19}H_{21}F_1N_8S$ 412.5; observed MH^+ (LCMS) 413.2 (m/z); ^{13}C NMR (125 MHz, DMSO-d_6) δ 163.1, 156.4, 144.1, 141.4, 137.9, 133.2, 130.0, 128.0, 122.7, 110.1, 109.3, 107.8, 85.3 (d, J = 114 Hz), 56.0, 47.7 (2C), 28.1 (d, J = 13 Hz, 2C), 20.7; HRMS (ESI) m/z obsd 413.1668 (M + H), calcd 413.1672.

***N*-[3-[(4,4-Difluoro-1-piperidinyl)methyl]-5-isothiazolyl]-6-methyl-3-(1*H*-pyrazol-4-yl)imidazo[1,2-*a*]pyrazin-8-amine Hydrochloride (11).** Following the general procedure, only substituting **5** with 4,4-difluoropiperdine hydrochloride, gave 140 mg (61% two-step yield) of the title compound (**11**) as an off-white solid. ^{1}H NMR (400 MHz, CD_3OD) δ 8.30−8.28 (m, 3H), 8.11 (s, 1H), 7.40 (s, 1H), 4.59 (s, 2H), 3.90−3.70 (m, 2H), 3.50−3.30 (m, 2H), 2.65 (s, 3H), 2.50−2.37 (m, 4H); mass calculated for formula $C_{19}H_{20}F_2N_8S$ 430.1; observed MH^+ (LCMS) 431.2 (m/z); ^{13}C NMR (125 MHz, CD_3OD) δ 163.0, 156.4, 153.8, 141.3, 138.2, 133.3, 129.7, 127.6, 122.7, 121.0 (t, J = 238 Hz), 110.2, 109.4, 109.3, 107.7, 55.0, 49.5 (2C), 31.2 (t, J = 25 Hz, 2C), 20.7; HRMS (ESI) m/z obsd 431.1578 (M + H), calcd 431.1577.

***N*-[3-[(3-Fluoro-1-piperidinyl)methyl]-5-isothiazolyl]-6-methyl-3-(1*H*-pyrazol-4-yl)imidazo[1,2-*a*]pyrazin-8-amine Hydrochloride (12).** Following the general procedure, only substituting **5** with 3-fluoropiperidine hydrochloride, gave 30 mg (69%, two-step yield) of the title compound (**12**) as an off-white solid. ^{1}H NMR (400 MHz, DMSO-d_6) δ 8.23−8.21 (m, 3H), 8.07 (s, 1H), 7.33 (s, 1H), 5.20−5.00 (m, 1H), 4.49 (bs, 2H), 4.00−3.80 (m, 2H), 3.80−3.60 (m, 2H), 2.63 (s, 3H), 2.30−2.10 (m, 2H), 2.00−1.80 (m, 2H); mass calculated for formula $C_{19}H_{21}F_1N_8S$ 412.5; observed MH^+ (LCMS) 413.2 (m/z); ^{13}C NMR (125 MHz, CD_3OD) δ 163.1, 161.0, 156.0, 150.9, 142.2, 137.8, 133.2, 129.9, 127.8, 122.7, 110.1, 109.3, 107.9, 86.0 (d, J = 113 Hz), 56.6, 54.3 (d, J = 25 Hz), 52.9, 25.9 (d, J = 25 Hz), 20.7, 18.2; HRMS (ESI) m/z obsd 413.1671 (M + H), calcd 413.1672.

***N*-[3-[(3,3-Difluoro-1-piperidinyl)methyl]-5-isothiazolyl]-6-methyl-3-(1*H*-pyrazol-4-yl)imidazo[1,2-*a*]pyrazin-8-amine Hydrochloride (13).** Following the general procedure, only substituting **5** with 3,3-difluoropiperidine hydrochloride, gave 20.0 mg (66%, two-step yield) of the title compound (**13**) as a beige solid. ^{1}H NMR (400 MHz, CD_3OD) δ 8.23−8.21 (app s, 3H), 8.09 (s, 1H), 7.37 (s, 1H), 4.60 (s, 2H), 3.90−3.70 (m, 2H), 3.60−3.40 (m, 2H), 2.64 (s, 3H), 2.35−2.10 (m, 4H); mass calculated for formula $C_{19}H_{20}F_2N_8S$ 430.5; observed MH^+ (LCMS) 431.2 (*m*/*z*), 92% pure by LCMS ; ^{13}C NMR (125 MHz, DMSO-d_6) δ 163.2, 155.8, 149.5, 141.7, 137.5, 133.2, 130.3, 128.9, 122.7, 120.3 (t, J = 238 Hz), 110.3, 109.3, 108.1, 56.2, 54.2 (t, J = 25 Hz), 51.6, 30.5 (t, J = 25 Hz), 20.7, 19.5; HRMS (ESI) *m*/*z* obsd 431.1573 (M + H), calcd 431.1578.

6-Methyl-3-(1*H*-pyrazol-4-yl)-*N*-[3-[[4-(trifluoromethyl)-1-piperidinyl]methyl]-5-isothiazolyl]imidazo[1,2-*a*]pyrazin-8-amine Hydrochloride (14). Following the general procedure, only substituting **5** with 4-(trifluoromethyl)piperidine hydrochloride, gave 156 mg (62%, two-step yield) of the title compound (**14**) as a light beige solid. ^{1}H NMR (400 MHz, CD_3OD) δ 8.27−8.25 (m, 3H), 8.10 (s, 1H), 7.37 (s, 1H), 4.50 (s, 2H), 3.81−3.78 (m, 2H), 3.25−3.19 (m, 2H), 2.75−2.65 (m, 1H), 2.64 (s, 3H), 2.23−2.19 (m, 2H), 1.94−1.91 (m, 2H); mass calculated for formula $C_{20}H_{21}F_3N_8S$ 462.5; observed MH^+ (LCMS) 463.3 (*m*/*z*); ^{13}C NMR (125 MHz, DMSO-d_6) δ 163.5, 156.0, 150.9, 142.1, 136.8, 132.9, 130.7 (q, J = 158 Hz), 126.8, 124.8, 122.6, 110.1, 109.2, 108.5, 56.3, 51.2, 48.5 (q, J = 21 Hz), 22.4, 20.7, 20.6; HRMS (ESI) *m*/*z* obsd 463.1635 (M + H), calcd 463.1640.

***N*-[3-[(3(*S*)-Fluoro-1-pyrrolidinyl)methyl]-5-isothiazolyl]-6-methyl-3-(1*H*-pyrazol-4-yl)imidazo[1,2-*a*]pyrazin-8-amine Hydrochloride (16).** Following the general procedure, only substituting **5** with (*S*)-3-fluoropyrrolidine hydrochloride, gave 0.50 g (81% two-step yield) of the title compound (**16**) as a light beige solid. ^{1}H NMR (400 MHz, CD_3OD) δ 8.29 (s, 1H), 8.26 (app s, 2H), 8.10 (s, 1H), 7.32 (s, 1H), 5.49 (d, J = 53.2 Hz, 1H), 4.64 (bs, 2H), 4.17−3.94 (m, 2H), 3.66−3.48 (m, 2H), 2.65 (s, 3H), 2.60−2.38 (m, 2H); mass calculated for formula $C_{18}H_{19}F_1N_8S$ 398.5; observed MH^+ (LCMS) 399.2 (*m*/*z*); ^{13}C NMR (125 MHz, CD_3OD) δ 162.5, 156.5, 151.1, 142.5, 138.7, 134.4, 126.1, 122.9, 121.3, 108.7, 108.5, 105.2, 91.9 (d, J = 175 Hz), 60.6 (d, J = 25 Hz), 55.1, 53.1, 31.0 (d, J = 20 Hz), 19.4; HRMS (ESI) *m*/*z* obsd 399.1510 (M + H), calcd 399.1516.

***N*-[3-[(3(*R*)-Fluoro-1-pyrrolidinyl)methyl]-5-isothiazolyl]-6-methyl-3-(1*H*-pyrazol-4-yl)imidazo[1,2-*a*]pyrazin-8-amine Hydrochloride (17).** Following the general procedure, only substituting **5** with (*R*)-3-fluoropyrrolidine hydrochloride, gave 245 mg (37%, two-step yield) of the title compound (**17**) as a light tan solid. ^{1}H NMR (400 MHz, CD_3OD) δ 8.23 (app s, 3H), 8.08 (s, 1H), 7.29 (s, 1H), 5.50 (d, J = 52 Hz, 1H), 4.64 (bs, 2H), 4.17−3.94 (m, 2H), 3.66−3.42 (m, 2H), 2.64 (s, 3H), 2.58−2.30 (m, 2H); mass calculated for formula $C_{18}H_{19}F_1N_8S$ 398.5; observed MH^+ (LCMS) 399.2 (*m*/*z*); ^{13}C NMR (125 MHz, CD_3OD) δ 162.4, 156.5, 148.9, 142.5, 138.7, 134.4, 126.1, 122.9, 121.2, 108.7, 108.5, 105.4, 92.0 (d, J = 163 Hz), 60.6 (d, J = 13 Hz), 55.1, 53.2, 31.1 (d, J = 38 Hz), 19.4; HRMS (ESI) *m*/*z* obsd 399.1516 (M + H), calcd 399.1516.

***N*-[3-[(3,3-Difluoro-1-pyrrolidinyl)methyl]-5-isothiazolyl]-6-methyl-3-(1*H*-pyrazol-4-yl)imidazo[1,2-*a*]pyrazin-8-amine Hydrochloride (18).** Following the general procedure, only substituting **5** with 3,3-difluoropyrrolidine hydrochloride, gave 259 mg (91%, two-step yield) of the title compound (**18**) as an off-white solid. ^{1}H NMR (400 MHz, CD_3OD) δ 8.08 (app s, 2H), 7.76 (s, 1H), 7.70 (s, 1H), 7.08 (s, 1H), 3.73 (s, 2H), 2.94 (t, J = 13 Hz, 2H), 2.84 (t, J = 7.0 Hz, 2H), 2.49 (s, 3H), 2.30 (tt, J = 22, 15 Hz, 2H); mass calculated for formula $C_{18}H_{18}F_2N_8S$ 416.5; observed MH^+ (LCMS) 417.2 (*m*/*z*); ^{13}C NMR (125 MHz, DMSO-d_6) δ 163.1, 156.7, 147.1, 141.5, 137.7, 133.1, 130.1, 128.4, 128.2 (t, J = 244 Hz), 122.7, 109.4, 109.3, 107.9, 58.9 (t, J = 38 Hz), 54.5, 52.6, 34.3 (t, J = 25 Hz), 20.7; HRMS (ESI) *m*/*z* obsd 417.1419 (M + H), calcd 417.1421.

6-Methyl-3-(1*H*-pyrazol-4-yl)-*N*-[3-[(3,3,4,4-tetrafluoro-1-pyrrolidinyl)methyl]-5-isothiazolyl]imidazo[1,2-*a*]pyrazin-8-amine Hydrochloride (19). Following the general procedure, only substituting **5** with 3,3,4,4-tetrafluoropyrrolidine hydrochloride, gave 16.3 mg (17%, two-step yield) of the title compound (**19**) as a light beige solid. ^{1}H NMR (400 MHz, CD_3OD) δ 8.29 (app s, 2 H), 8.22 (s, 1H), 8.10 (s, 1H), 7.13 (s, 1H), 3.88 (bs, 2H), 3.32 (t, J = 13 Hz, 4H), 2.49 (s, 3H); mass calculated for formula $C_{18}H_{16}F_4N_8S$ 452.4; observed MH^+ (LCMS) 453.2 (*m*/*z*); ^{13}C NMR (125 MHz, DMSO-d_6) δ 162.7, 161.9, 153.2, 140.8, 138.7, 133.5, 129.2, 126.5, 122.8, 120.3 (tt, J = 262, 26 Hz, 2C), 109.3, 108.2, 107.4, 58.6 (t, J = 25 Hz), 54.7, 20.6; HRMS (ESI) *m*/*z* obsd 453.1247 (M + H), calcd 453.1233.

***N*-[3-[(3-Fluoro-1-azetidinyl)methyl]-5-isothiazolyl]-6-methyl-3-(1*H*-pyrazol-4-yl)imidazo[1,2-*a*]pyrazin-8-amine Trifluoroacetate (20).** Following the general procedure, only substituting **5** with 3-fluoroazetidine trifluoroacetate and substituting NaH with Na_2CO_3, gave 40.9 mg (64%, two-step yield) of (**20**) as a light beige solid. ^{1}H NMR (400 MHz, DMSO-d_6) δ 12.3 (broad s, NH), 8.50 (s, 1H), 8.28 (broad s, NH), 8.08 (s, 1H), 7.97 (s, 1H), 7.90 (s, 1H), 7.18 (s, 1H), 5.47−5.35 (m, 3H), 4.65−4.43 (m, 2H), 4.41−4.25 (m, 2H), 2.47 (s, 3H); mass calculated for formula $C_{17}H_{17}F_1N_8S$ 384.4; observed MH^+ (LCMS) 385.2 (*m*/*z*); ^{13}C NMR (125 MHz, DMSO-d_6) δ 163.6, 157.0, 151.3, 142.5, 138.6, 136.3, 131.7, 128.5, 122.0, 110.0, 109.1, 107.9, 84.7 (d, J = 125 Hz), 74.7, 62.0 (d, J = 25 Hz), 20.7; HRMS (ESI) *m*/*z* obsd 385.1361 (M + H), calcd 385.4418.

***N*-[3-[(3,3-Difluoro-1-azetidinyl)methyl]-5-isothiazolyl]-6-methyl-3-(1*H*-pyrazol-4-yl)imidazo[1,2-*a*]pyrazin-8-amine Trifluoroacetate (21).** Following the general procedure, only substituting **5** with 3,3-difluoroazetidine hydrochloride and substituting NaH with K_2CO_3, gave 49.8 mg (17%, two-step yield) of (**21**) as a white solid. ^{1}H NMR (400 MHz, CD_3OD) δ 8.10 (bs, 2H), 7.77 (s, 1H), 7.71 (s, 1H), 7.04 (s, 1H), 3.84 (s, 2H), 3.74 (t, J = 12 Hz, 4H), 2.49 (s, 3H); mass calculated for formula $C_{17}H_{16}F_2N_8S$ 402.1; observed MH^+ (LCMS) 403.2 (*m*/*z*); ^{13}C NMR (125 MHz, DMSO-d_6) δ 163.3, 159.0, 158.0, 142.4, 136.2, 131.5 (3C), 122.5, 109.1, 108.8, 108.4, 107.9 (t, J = 243 Hz), 108.4, 65.3 (t, J = 25 Hz), 56.0, 20.7; HRMS (ESI) *m*/*z* obsd 403.1254 (M + H), calcd 403.1265.

6-Methyl-3-(1*H*-pyrazol-4-yl)-*N*-[3-[[(3,3,3-trifluoropropyl)-amino]methyl]-5-isothiazolyl]imidazo[1,2-*a*]pyrazin-8-amine Hydrochloride (22). Following the general procedure, only substituting **5** with 3,3,3-trifluoropropylamine, gave 18.8 mg (38%, two-step yield) of the title compound (**22**) as an off-white solid. ^{1}H NMR (400 MHz, CD_3OD) δ 8.18 (app s, 2H), 8.05 (s, 1H), 7.99 (s, 1H), 7.20 (s, 1H), 4.44 (s, 2H), 3.50−3.40 (m, 2H), 2.85−2.70 (m, 2H), 2.60 (s, 3H); mass calculated for formula $C_{17}H_{17}F_3N_8S$ 422.4; observed MH^+ (LCMS) 423.2 (*m*/*z*); ^{13}C NMR (125 MHz, DMSO-d_6) δ 163.2, 157.8, 151.3, 141.8, 137.3, 133.0, 130.6, 130.0 (q, J = 217 Hz), 125.6, 122.6, 109.2, 108.2, 108.1, 55.5, 47.8, 30.6 (q, J = 29 Hz), 20.7; HRMS (ESI) *m*/*z* obsd 423.1335 (M + H), calcd 423.1327.

6-Methyl-*N*-[3-[[(2,2,3,3,3-pentafluoropropyl)amino]methyl]-5-isothiazolyl]-3-(1*H*-pyrazol-4-yl)imidazo[1,2-*a*]pyrazin-8-amine Hydrochloride (23). Following the general procedure, only substituting **5** with 2,2,3,3,3-pentafluoropropylamine, gave 49.7 mg (49%, two-step yield) of the title compound (**23**) as an off-white solid. ^{1}H NMR (400 MHz, CD_3OD) δ 8.22 (app s, 2H), 8.18 (s, 1H), 8.06 (s, 1H), 7.28 (s, 1H), 4.56 (s, 2H), 4.24 (t, J = 16 Hz, 2H), 2.63 (s, 3H); mass calculated for formula $C_{17}H_{15}F_5N_8S$ 458.4; observed MH^+ (LCMS) 459.3 (*m*/*z*); ^{13}C NMR (125 MHz, DMSO-d_6) δ 162.9, 158.1, 150.0, 141.6, 137.7, 133.2, 130.2, 128.5, 122.7, 118.8 (q, J = 308 Hz), 113.6 (t, J = 188 Hz), 109.3, 108.5, 107.9, 48.7, 45.4 (t, J = 19 Hz), 20.7; HRMS (ESI) *m*/*z* obsd 459.1141 (M + H), calcd 459.1139.

Deuterated (5-(6-Methyl-3-(1-((2-(trimethylsilyl)ethoxy)methyl)-1*H*-pyrazol-4-yl)imidazo[1,2-*a*]pyrazin-8-ylamino)isothiazol-3-yl)-methyl-(d2) Methanesulfonate (24). A flask was charged with lithium aluminum deuteride (0.98 g, 23.3 mmol). Anhydrous THF was added (40 mL). A solution of **2** (2.06 g, 4.25 mmol) in anhydrous THF (60 mL) was carefully added to the reaction flask.

The resulting mixture was stirred at room temperature under a N_2 atmosphere for 1.0 h. The reaction was carefully quenched by the sequential addition of 0.98 mL of H_2O, 0.98 mL of 15% NaOH (aq), and 2.94 mL H_2O. After being stirred for 10 min, the mixture was filtered through a very thin pad of Celite (rinsing with THF). Concentration of the filtrate yielded a light yellow solid. Triturating with MeOH gave the pure alcohol (0.96 g, 49% yield) as a white solid. ^{1}H NMR (400 MHz, $CDCl_3$) δ 9.81 (s, NH), 7.88 (s, 1H), 7.81 (s, 1H), 7.60 (s, 1H), 7.49 (s, 1H), 6.90 (s, 1H), 5.54 (s, 2H), 3.67 (t, J = 8.2 Hz, 2H), 2.51 (s, 3H), 0.96 (t, J = 8.2 Hz, 2H), 0.0 (s, 9H); mass calculated for formula $C_{20}H_{25}D_2N_7O_2SSi$ 459.2; observed MH^+ (LCMS) 460.4 (m/z); ^{13}C NMR (125 MHz, $CDCl_3$) δ 166.2, 162.0, 142.3, 139.1, 137.6, 132.1, 131.6, 128.4, 120.8, 110.7, 107.6, 105.7, 81.1, 67.8, 61.3, 20.9, 18.3, −1.0 (3C); HRMS (ESI) m/z obsd 460.1918 (M + H), calcd 460.1920.

A solution of the alcohol (1.57 g, 3.42 mmol) in THF (171 mL) was treated with Et_3N (1.7 mL, 11.96 mmol) followed by methanesulfonyl chloride (0.7 mL, 8.54 mmol). The mixture was stirred at room temperature for 5 min, and then water (100 mL) was added. Dichloromethane (200 mL) was added, and the layers were separated. The organic phase was washed with 1.0 N HCl (aq), saturated $NaHCO_3$ (aq), and brine. The organic phase was dried over Na_2SO_4, filtered, and concentrated in vacuo to give an off-white solid. Triturating with MeOH gave pure **24** (1.13 g, 62% yield) as a white solid; ^{1}H NMR (400 MHz, $CDCl_3$) δ 7.92 (s, 1H), 7.84 (s, 1H), 7.65 (s, 1H), 7.54 (s, 1H), 7.06 (s, 1H), 5.55 (s, 2H), 3.68 (t, J = 8.2 Hz, 2H), 3.05 (s, 3H), 2.55 (s, 3H), 0.95 (t, J = 8.2 Hz, 2H), 0.01 (s, 9H); mass calculated for formula $C_{21}H_{27}D_2N_7O_4S_2Si$ 537.2; observed MH^+ (LCMS) 538.3 (m/z); ^{13}C NMR (125 MHz, $CDCl_3$) δ 162.9, 158.8, 142.2, 139.1, 137.8, 131.9, 131.4, 128.9, 121.2, 110.3, 107.9, 107.3, 81.1, 67.8, 64.4, 38.6, 20.9, 18.3, −1.0 (3C); HRMS (ESI) m/z obsd 538.1693 (M + H), calcd 538.1695.

Deuterated *N*-[3-[(3,3-Difluoro-1-pyrrolidinyl)methyl-(d2)]-5-isothiazolyl]-6-methyl-3-(1*H*-pyrazol-4-yl)imidazo[1,2-*a*]pyrazin-8-amine Hydrochloride (25). Following the general procedure, using 3,3-difluoropyrrolidine hydrochloride and mesylate **24**, 37.1 mg (69%, two-step yield) was obtained of the title compound (**25**) as an off-white solid. ^{1}H NMR (400 MHz, CD_3OD) δ 8.27 (app s, 2H), 8.25 (s, 1H), 8.09 (s, 1H), 7.32 (s, 1H), 4.07−4.00 (m, 2H), 3.95−3.83 (m, 2H), 2.80−2.63 (m, 2H), 2.64 (s, 3H); mass calculated for formula $C_{18}H_{16}D_2F_2N_8S$ 418.5; observed MH^+ (LCMS) 419.2 (m/z); ^{13}C NMR (125 MHz, DMSO-d_6) δ 162.5, 156.8, 140.5, 139.4, 133.6, 128.4 (t, J = 250 Hz), 125.1, 122.9, 109.6, 109.3, 107.0, 58.7 (t, J = 38 Hz), 53.7, 52.4, 34.4 (t, J = 19 Hz), 20.7; HRMS (ESI) m/z obsd 419.1556 (M + H), calcd 419.1547.

Deuterated 6-Methyl-*N*-[3-(1-piperidinylmethyl-(d2))-5-isothiazolyl]-3-(1*H*-pyrazol-4-yl)imidazo[1,2-*a*]pyrazin-8-amine Hydrochloride (26). Following the general procedure, using piperidine and mesylate **24**, 60.9 mg (89%, two-step yield) was obtained of the title compound (**26**) as an off-white solid. ^{1}H NMR (400 MHz, CD_3OD) δ 8.23 (s, 2H), 8.21 (s, 1H), 8.07 (s, 1H), 7.33 (s, 1H), 3.63 (t, J = 2.7 Hz, 2H), 3.09 (t, J = 3.7 Hz, 2H), 2.63 (s, 3H), 1.94 (m, 2H); mass calculated for formula $C_{19}H_{20}D_2N_8S$ 396.5; observed MH^+ (LCMS) 397.2 (m/z); ^{13}C NMR (125 MHz, CD_3OD) δ 163.1, 156.3, 147.8, 141.5, 137.6, 133.9 (2C), 130.2, 128.7, 110.3, 109.3 (2C), 53.1 (2C), 49.6, 23.2 (2C), 22.3, 20.9; HRMS (ESI) m/z obsd 397.1906 (M + H), calcd 397.1892.

Deuterated 6-Methyl-3-(1*H*-pyrazol-4-tl)-*N*-[3-[[(3,3,3-trifluoropropyl)amino]methyl-(d2)]-5-isothiazolyl]imidazo[1,2-*a*]pyrazin-8-amine Hydrochloride (27). Following the general procedure, using 3,3,3-trifluoropropylamine hydrochloride and mesylate **24**, 21.9 mg (68%, two-step yield) was obtained of the title compound (**27**) as an off-white solid. ^{1}H NMR (400 MHz, CD_3OD) δ 8.25 (s, 2H), 8.23 (s, 1H), 8.08 (s, 1H), 7.28 (s, 1H), 3.47 (t, J = 1.95 Hz, 2H), 2.79 (m, 2H), 2.64 (s, 3H); mass calculated for formula $C_{17}H_{15}D_2F_3N_8S$ 424.4; observed MH^+ (LCMS) 425.2 (m/z); ^{13}C NMR (125 MHz, DMSO) δ 163.1, 157.6, 152.2, 141.3, 138.0, 133.1 (broad s, 2C), 127.9 (q, J = 288 Hz), 122.6, 109.1, 107.9, 107.8, 60.5, 30.5 (q, J = 29.1 Hz), 20.4.

Biochemical Assays. Aurora A and Aurora B kinase assays were performed in low protein binding 384-well plates. Compounds were diluted in 100% DMSO to the desired concentrations. For the Aurora A assay, each sample consisted of 8 nM enzyme (Aurora A, Upstate), 100 nM Tamra-PKAtide (Molecular Devices, 5TAMRA-GRTGRRNSICOOH), 25 μM ATP, 1 mM DTT, and kinase buffer (10 mM Tris, 10 mM $MgCl_2$, 0.01% Tween 20). For the Aurora B assay, each sample consisted of 26 nM enzyme (Aurora B, Invitrogen), 100 nM Tamra-PKAtide (Molecular Devices, 5TAMRA-GRTGRRNSICOOH), 50 μM ATP, 1 mM DTT, and kinase buffer (10 mM Tris, 10 mM $MgCl_2$, 0.01% Tween 20). Dose-response curves were plotted from inhibition data generated in duplicate, from eight-point serial dilutions of inhibitory compounds. Concentration of compound was plotted against kinase activity, calculated by degree of fluorescent polarization. To generate IC_{50} values, the dose-response curves were then fitted to a standard sigmoidal curve and IC_{50} values were derived by nonlinear regression analysis.

Histone H3 Phosphorylation Assay. HCT-116 cells were plated at 15 000 cells per well in poly-D-lysine coated black microclear 384-well tissue culture plates. For the phos-Histone H3 assay, cells were first treated with 0.4 mg/mL nocodazole for 16 h. Subsequently, cells were treated for 1 h with compound (0.1% final DMSO concentration) in triplicate wells. Cells were fixed with Prefer fixation solution (Anatech) plus 1000 nM Hoechst 33342 dye and incubated for 30 min at room temperature. The fixation solution was removed, and cells were washed with PBS. Cells were permeabilized with 0.2% Triton-X in PBS and incubated for 10 min. Cells were washed with PBS and incubated with PBS containing 3% FBS for 30 min. Cells were then stained overnight at 4 °C with phos-Histone H3 (ser10)-Alexa Fluor 488 conjugate antibody (Cell Signaling) solution in PBS plus 3% FBS. Cells were washed with PBS, and then immunofluorescence images were captured at 10× using the BD Pathway 855 automated fluorescent microscope (BD Bioscience). Percent positive cells was quantitated by Hoechst staining for total cell number using Attovision software (BD Bioscience). To generate IC_{50} values, the dose-response curves were then fitted to a standard sigmoidal curve and IC_{50} values were derived by nonlinear regression analysis.

In Vivo Pharmacology: Pharmacodynamic Biomarker Activity in A2780 Human Tumor Xenograft. Nu/nu mice (female, 5−7 weeks of age) were injected subcutaneously with 5×10^6 A2780 cells/mouse. When tumor cells reached approximately 200−500 mm^3, mice were randomly grouped into treatment groups (n = 3). Animals were dosed through oral gavage. The compound was dissolved in 20% hydroxylpropyl-β-cyclodextrin. Tumors were excised from the animals 2 h after a single dose of the compound, and the tissue was fixed in 10% buffered formaldehyde for 24 h and then trimmed to equal size (~75 mm^3) and processed for paraffin embedding using a 30 min cycle on a tissue processing instrument (Sakura Tissue-Tek VIP). Processed tissues were embedded in paraffin blocks. Then 5 μm thick sections were cut on microtome and mounted onto positive charged slides, deparaffinized, rehydrated, and subjected to antigen retrieveal in Target Retrieval Solution (Dako) using the Black and Decker steamer (98 °C for 35 min.). Sections were then incubated in 3% hydrogen peroxide for 5 min at room temperature (RT), rinsed in Tris buffered saline with 0.05% Tween 20 (TBST), incubated with rabbit polyclonal antibody against phospho-Histone H3 (Ser 10) (Millipore catalog nu. 06-567) for 30 min at RT, rinsed in TBST buffer, subjected to detection reaction using the EnVision$^+$ HRP polymer detection system (Dako) for 30 min at RT, rinsed in TBST, and incubated in 3,3′-diaminobenzidine (DAB) for 5 min at RT. Finally, the sections were counterstained with Gill 2 hematoxylin. Ten consecutive fields of positive area were imaged at 40× for analysis from each tumor sample. Image-Pro image analysis program is used to analyze IHC assay.

Acknowledgment. We thank Drs. William Greenlee, Malcolm MacCoss, Paul Kirschmeier, Dan Hicklin, and W. Robert Bishop for their support. We express our gratitude to Dr. Jesse Wong (Discovery Prep Group) and Dr. Mathew Rainka (AMRI) for supplying large amounts of compound **2**. Li-Kang Zhang, Ross Yang, Ibrahim Daaro (Mass Spectrometry) and Alan Hruza and Johannes Voigt (Structural Chemistry) are all appreciatively acknowledged for their supporting studies.

References

(1) Kimura, M.; Matsuda, Y.; Yoshioka, T.; Okano, Y. Cell cycle-dependent expression and centrosome localization of a third human aurora/Ipl1-related protein kinase, AIK3. *J. Biol. Chem.* **1999**, *274*, 7334–7340.

(2) Tanaka, T.; Kimura, M.; Matsunaga, K.; Fukada, D.; Mori, H.; Okano, Y. Centrosomal kinase AIK1 is overexpressed in invasive ductal carcinoma of the breast. *Cancer Res.* **1999**, *59*, 2041–2044.

(3) Reiter, R.; Gais, P.; Jütting, U.; Steuer-Vogt, M. K.; Pickhard, A.; Bink, K.; Rauser, S.; Lassmann, S.; Höfler, H.; Werner, M.; Walch, A. Aurora kinase A messenger RNA overexpression is correlated with tumor progression and shortened survival in head and neck squamous cell carcinoma. *Clin. Cancer Res.* **2006**, *12*, 5136–5141.

(4) Gritsko, T. M.; Coppola, D.; Paciga, J. E.; Yang, L.; Sun, M.; Shelley, S. A.; Fiorica, J. V.; Nicosia, S. V.; Cheng, J. Q. Activation and overexpression of centrosome kinase BTAK/Aurora-A in human ovarian cancer. *Clin. Cancer Res.* **2003**, *9*, 1420–1426.

(5) Lee, E. C.; Frolov, A.; Li, R.; Ayala, G.; Greenberg, N. M. Targeting Aurora kinases for the treatment of prostate cancer. *Cancer Res.* **2006**, *66*, 4996–5002.

(6) Sen, S.; Zhou, H.; Zhang, R. D.; Yoon, D. S.; Vakar-Lopez, F.; Ito, S.; Jiang, F.; Johnston, D.; Grossman, H. B.; Ruifrok, A. C.; Katz, R. L.; Brinkley, W.; Czerniak, B. Amplification/overexpression of a mitotic kinase gene in human bladder cancer. *J. Natl. Cancer Inst.* **2002**, *94*, 1320–1329.

(7) Tanaka, E.; Hashimoto, Y.; Ito, T.; Okumura, T.; Kan, T.; Watanabe, G.; Imamura, M.; Inazawa, J.; Shimada, Y. The clinical significance of Aurora-A/STK15/BTAK expression in human esophageal squamous cell carcinoma. *Clin. Cancer Res.* **2005**, *11*, 1827–1834.

(8) Ulisse, S.; Delcros, J. G.; Baldini, E.; Toller, M.; Curcio, F.; Giacomelli, L.; Prigent, C.; Ambesi-Impiombato, F. S.; D'Armiento, M.; Arlot-Bonnemains, Y. Expression of Aurora kinases in human thyroid carcinoma cell lines and tissues. *Int. J. Cancer* **2006**, *119*, 275–282.

(9) Zeng, W. F.; Navaratne, K.; Prayson, R. A.; Weil, R. J. Aurora B expression correlates with aggressive behaviour in glioblastoma multiforme. *J. Clin. Pathol.* **2007**, *60*, 218–221.

(10) Bischoff, J. R.; Anderson, L.; Zhu, Y.; Mossie, K.; Ng, L.; Souza, B.; Schryver, B.; Flanagan, P.; Clairvoyant, F.; Ginther, C.; Chan, C. S. M.; Novotny, M.; Slamon, D. J.; Plowman, G. D. A homologue of Drosophila aurora kinase is oncogenic and amplified in human colorectal cancers. *EMBO J.* **1998**, *17*, 3052–3065.

(11) Murnion, M. E.; Adams, R. R.; Callister, D. M.; Allis, C. D.; Earnshaw, W. C.; Swedlow, J. R. Chromatin-associated protein phosphatase 1 regulates aurora-B and histone H3 phosphorylation. *J. Biol. Chem.* **2001**, *276*, 26656–26665.

(12) Yang, H.; Burke, T.; Dempsey, J.; Diaz, B.; Collins, E.; Toth, J.; Beckmann, R.; Ye, X. Mitotic requirement for aurora A kinase is bypassed in the absence of aurora B kinase. *FEBS Lett.* **2005**, *579*, 3385–3391.

(13) Basso, A. D.; Liu, M.; Gray, K.; Tevar, S.; Liang, L.; Ponery, A.; Smith, E. B.; Monsma, F. J.; Yu, T.; Zhang, Y.; Kerekes, A. D.; Esposite, S.; Xiao, Y.; Tagat, J. R.; Hicklin, D. J.; Kirschmeier, P. SCH 1473759, a Novel Aurora Inhibitor, Demonstrates Enhanced Antitumor Activity in Combination with Taxanes and KSP Inhibitors. Unpublished results.

(14) Yu, T.; Tagat, J. R.; Kerekes, A. D.; Doll, R. J.; Zhang, Y.; Xiao, Y.; Esposite, S. J.; Belanger, D.; Curran, P.; Mandal, A. K.; Siddiqui, A. M.; Shih, N.-Y.; Basso, A. D.; Liu, M.; Gray, K.; Tevar, S.; Jones, J.; Lee, S.; Liang, L.; Ponery, S.; Smith, E. B.; Hruza, A.; Voigt, J.; Ramanathan, L.; Prosise, W.; Hu, M. Discovery of a potent, injectable inhibitor of Aurora kinases based on the imidazo-[1,2-*a*]-pyrazine core. *ACS Med. Chem. Lett.* **2010**, *1*, 214–218.

(15) Müller, K.; Faeh, C.; Diederich, F. Fluorine in pharmaceuticals: looking beyond intuition. *Science* **2007**, *317*, 1881–1886.

(16) Böhm, H.-J.; Banner, D.; Bendels, S.; Kansy, M.; Kuhn, B.; Müller, K.; Obst-Sander, U.; Stahl, M. Fluorine in medicinal chemistry. *ChemBioChem* **2004**, *5*, 637–643.

(17) Hagmann, W. K. The many roles for fluorine in medicinal chemistry. *J. Med. Chem.* **2008**, *51*, 4359–4369.

(18) Morganthaler, M.; Schweizer, E.; Hoffmann-Röder, A.; Benin, F.; Martin, R. E.; Jaeschke, G.; Wagner, B.; Fischer, H.; Bendels, S.; Zimmerli, D.; Schneider, J.; Diederich, F.; Kansy, M.; Müller, K. Predicting and tuning physicochemical properties in lead optimization: amine basicities. *ChemMedChem* **2007**, *2*, 1100–1115.

(19) Van Neil, M. B.; Collins, I.; Beer, M. S.; Broughton, H. B.; Cheng, S. K. F.; Goodacre, S. C.; Heald, A.; Locker, K. L.; MacLeod, A. M.; Morrison, D.; Moyes, C. R.; O'Conner, D.; Pike, A.; Rowley, M.; Russell, M. G. N.; Sohal, B.; Stanton, J. A.; Thomas, S.; Verrier, H.; Watt, A. P.; Castro, J. L. Fluorination of 3-(3-(piperidin-1-yl)propyl)indoles and 3-(3-(piperazin-1-yl)propyl)-indoles gives selective human 5-HT_{1D} receptor ligands with improved pharmacokinetic profiles. *J. Med. Chem.* **1999**, *42*, 2087–2104.

(20) Yu, T.; Belanger, D.; Kerekes, A. D.; Meng, Z.; Tagat, J. R.; Esposite, S. J.; Mandel, A. K.; Xiao, Y.; Kulkarni, B. A.; Zhang, Y.; Curran, P. J.; Doll, R.; Siddiqui, M. A. Imidazopyrazines as Protein Kinase Inhibitors and Their Preparation and Use in the Treatment of Kinase-Mediated Diseases. WO 2008156614, 2008; 287 pp.

(21) Murnion, M. E.; Adams, R. R.; Callister, D. M.; Allis, C. D.; Earnshaw, W. C.; Swedlow, J. R. Chromatin-associated protein phosphatase 1 regulates aurora-B and histone H3 phosphorylation. *J. Biol. Chem.* **2001**, *276*, 26656–26665.

(22) Korfmacher, W. A.; Cox, K. A.; Ng, K. J.; Veals, J.; Hsien, Y.; Wainhaus, S.; Broske, L.; Prelusky, D.; Nomeir, A.; White, R. E. Cassette-accelerated rapid rat screen: a systematic procedure for the dosing and liquid chromatography/atmospheric pressure ionization tandem mass spectrometric analysis of new chemical entities as part of new drug discovery. *Rapid Commun. Mass. Spectrom.* **2001**, *15*, 335–340.

(23) Wilberg, K. B. The deuterium isotope effect. *Chem. Rev.* **1955**, *55*, 713.

(24) Pollard, J. R.; Mortimore, M. Discovery and development of Aurora kinase inhibitors as anticancer agents. *J. Med. Chem.* **2009**, *52*, 2629–2651.